Dyes and Pigments 108 (2014) 76–83

Contents lists available at ScienceDirect

Dyes and Pigments

journal homepage: www.elsevier.com/locate/dyepig

Ratiometric double channel borondipyrromethene based chemodosimeter for the selective detection of nerve agent mimics

R. Gotor, A.M. Costero*, P. Gaviña, Salvador Gil

Centro de Reconocimiento Molecular y Desarrollo Tecnológico, Unidad Mixta Universidad Politécnica de Valencia – Universidad de Valencia and Departamento de Química Orgánica, Universidad de Valencia, C/Dr. Moliner 50, 46100 Burjassot, Valencia, Spain

ARTICLE INFO

Article history:
Received 24 February 2014
Received in revised form
4 April 2014
Accepted 5 April 2014
Available online 25 April 2014

Keywords:
Nerve agents
Chemodosimeter
Gas
BODIPY
Fluorescence
naked-eye

ABSTRACT

A new chromo-fluorogenic probe based on the borondipyrromethene dye has been synthesized. The dye has been attached to a sensing unit for the diethylcyanophosphonate and di-isopropylfluorophosphate detection. The new probe has been fully characterized, and its optical properties in front of these simulants have been evaluated. No interference from other organo-phosphorous or other common contaminants compounds has been observed in the detection conditions. A portable kit has been developed and tested to demonstrate its practical application in real-time monitoring not only in solution but also in gas phase.

1. Introduction

The international concern on the power of destruction of the denominated chemical warfare has been raised in the last decades. Threats of chemical warfare attacks are increasingly more common at every war conflict, being used even as war propaganda. The very well known nerve agents Sarin, Soman and Tabun are popular among armies and terrorist groups [1]. Their extreme toxicity, together with their low cost and ease of production makes these compounds a big concern for governments and civilians.

Due to the chemical nature of the nerve agents, *i.e.* organophosphorous derivatives with a good leaving group (Scheme 1), they irreversibly bind to a free serine residue of acetylcholinesterase, inhibiting its enzymatic task [2]. After intoxication, acetylcholine is over-accumulated in the synaptic junctions of the nerves. The disorder has immediate effects: muscle relaxation hindering, hyperventilation and death in the cases of high exposure. Even if some antidotes have proven to reduce the effects of the over-accumulation of acetylcholine (atropine) or to reactivate the enzymatic task of acetylcholinesterase [3], they urge to be applied within few minutes after intoxication. Therefore the need of sensing these agents soon after any leakage is more than justified.

The detection and monitoring of these compounds has been accomplished by means of different technologies: ion mobility spectroscopy [4], mass spectrometry [5] and proton transfer mass spectrometry [6] biosensors [7], electrochemical methods [8], microcantilevers [9], photonic crystals [10], optical-fibre arrays [11], and nanomaterials such as nanotubes or nanowires [12]; but most of them have several drawbacks such as complexity, low portability, high costs or the need of qualified personal to operate the devices.

The use of chemodosimeters for in-field detection has recently gained importance due to economical and practical factors considering that the required instrumentation as well as their synthesis has proved to be cost-effective and portable, providing even semiquantitative analysis by the “naked-eye”.

Among the existing probes for nerve agents, the transduction mechanism usually involves intramolecular charge transfer (ICT) [13], photoinduced electron transfer (PET) [14a], or Förster resonance electron transfer (FRET) processes [15], as well as plasmon band of gold nanoparticles [16], discolouration of coordination complexes [17] or a mixture of them suited for colourimetric arrays [18].

Within our nerve agents detection research, we have developed diverse sensing units that became part of chromophores

* Corresponding author.
E-mail address: ana.costero@uv.es (A.M. Costero).

http://dx.doi.org/10.1016/j.dyepig.2014.04.011
0143-7208/

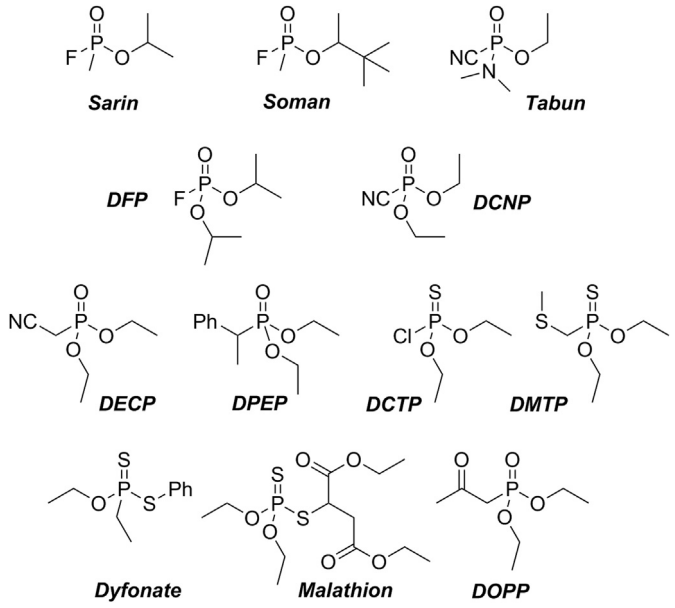

Scheme 1. Chemical structures of the nerve agents Sarin, Soman, and Tabun, their simulants diisopropylfluorophosphate (DFP) and diethylcyanophosphonate (DCNP), and other potential interferents.

such as stilbenes or triarylmethane dyes [13]. Other authors opted for the fluorogenic sensing, employing pyrene or biphenyl dyes [14].

The reputation of borondipyrromethene (BODIPY) dyes in sensing and fluorescent labelling applications, energy transfer cassettes or laser dyes among others has grown considerably [19]. It is not surprising if one considers its outstanding optical properties, such as high and environment-independent quantum yields, strong extinction coefficients and photostability, together with the ease of synthesis and functionalization (Table 1).

With the aim of developing a sensible, selective and high stable chemical warfare chemodosimeter, we have decided to synthesize the BODIPY based probe **1**, (see Scheme 2) bearing a 2-(2-(dimethylamino)phenyl)ethanol sensing unit, which has already proved to give good results regarding sensitivity and selectivity towards nerve agent simulants [13a].

In the presence of nerve gases, the 2-(2-(dimethylamino) phenyl)ethanol unit, reacts with the organophosphorous compound through the hydroxyl group forming a phosphoester, which in a second step is displaced by the nucleophilic attack of the nitrogen atom in an intramolecular cyclisation reaction, forming a quaternary ammonium salt.

The sensing unit was decided to be electronically connected to the BODIPY core in order to have a two optic channel chemodosimeter. We expected that the energy of the extended π-system could be modulated through an ICT process upon analyte detection, which would turn into a modulation in the absorption and emission properties of the dye.

Table 1
Spectroscopic properties of probe **1** and $1 + H^+$ (5×10^{-6} M in MeCN). $\lambda_{exc} = 480$ nm. Φ_f was measured Rhodamine 6G as standard [23].

Compound	λ_{abs} (nm)	λ_{em} (nm)	Φ_f	τ_1 (ps)	τ_2 (ps)
1	530	555	0.0006	[a]	[a]
1 + H^{+} [b]	524	555	0.639	230	4198

[a] Not measured due to low emission.
[b] Proton source is TFA.

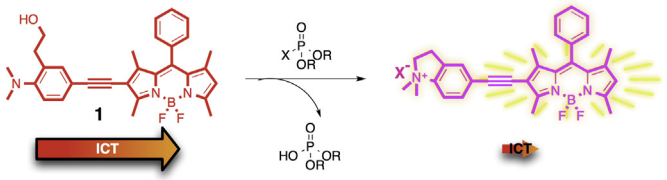

Scheme 2. Probe **1** and schematic representation of its reactivity towards some organophosphorous compounds.

2. Results and discussion

2.1. Synthesis of the probe

Probe **1** was synthesized by means of a Sonogashira cross-coupling between a bromo derivative of the *meso-phenyl* BODIPY dye and the sensing unit, functionalized with an ethynyl moiety. The synthesis of the sensing unit **4** began with the catalytic hydrogenation of 2-(2-nitrophenyl)ethanol in the presence of formaldehyde and Pd/C. This step was followed by aromatic bromination of the resulting 2-(2-dimethylaminophenyl)ethanol with NBS catalysed with ammonium acetate to form **2**. A Sonogashira cross-coupling reaction between **2** and trimethylsilylacetylene yielded the compound **3**, which was deprotected prior to use in a mixture of K_2CO_3 in methanol to finally yield the sensing unit **4** (see Scheme 3).

Bromination of dye **5** was performed using one equivalent of NBS in a DMF/DCM solvent mixture, yielding 60% of dye **6**. Dye **5** was previously synthesized from the condensation of 2,4-dimethylpyrrole and benzaldehyde, followed by oxidation with DDQ and reaction with $BF_3 \cdot Et_2O$ as reported in the literature [20]. Finally, compound **4** was coupled with the 2-bromo BODIPY derivative **6** in a Sonogashira cross-coupling reaction, using $Pd(PPh_3)_4$ as catalyst in toluene/Et_3N mixtures.

2.2. Spectroscopic properties

The absorption spectrum of probe **1** was recorded in acetonitrile (5×10^{-6} M, see Fig. 1). The probe showed two weak absorptions at *ca.* 415 and 310 nm, together with an intense broad absorption band (ε = 36,800 cm^{-1} M^{-1}) in the visible region, centred at 530 nm, corresponding to the $S_0 \rightarrow S_1$ ($\pi \rightarrow \pi^*$) electronic transition.

This 33 nm red shift compared to that of parent BODIPY **5** (λ_{abs} = 497 nm, λ_{em} = 505 nm) follows the trend observed with

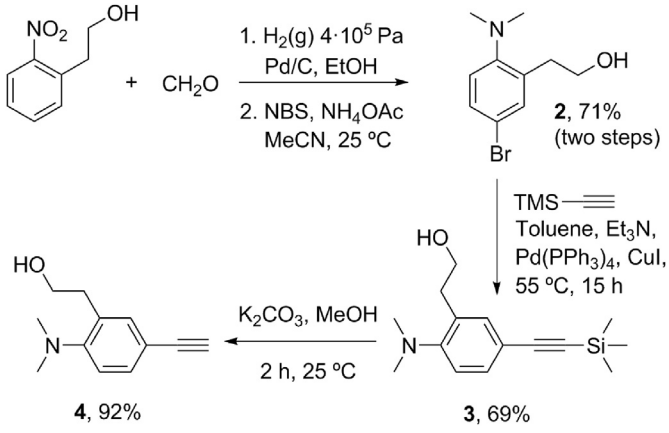

Scheme 3. Synthesis of the sensing unit **4**.

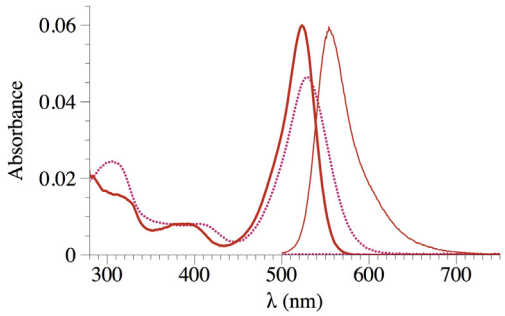

Fig. 1. Absorption and normalized emission spectra of probe **1** in acetonitrile (5×10^{-6} M) in the absence (dotted line) and in the presence of 5 mM of TFA ($\lambda_{exc} = 470$ nm).

other 2,6-arylethynyl substituted BODIPYs [21]. The shift can be ascribed mainly to the extension of the π-system, together with the formation of an internal charge transfer (ICT) system between the dimethylaniline-ethynyl donor moiety and the BODIPY acceptor core, lowering the HOMO-LUMO energy gap. It is worth to remark that this class of donor-ethynyl substituted BODIPYs is scarce in the literature [21,22], and most of the time consists in symmetrically 2,6-disubstituted BODIPYs forming a donor-acceptor-donor system.

If the donor group is deactivated (*i.e.* protonation of the dimethylaniline ethynyl moiety with TFA) a 6 nm hypsochromic shift of the main absorption band is observed together with a narrowing of the band. Moreover, a slight shoulder can be then observed at *ca.* 495 nm, presumably corresponding to the vibronic (0 → 1) transition of the $S_0 \rightarrow S_1$ electronic transition.

The emission spectrum of **1** has a band peaking at 555 nm with very low fluorescence quantum yield ($\Phi_f = 0.006$, using Rhodamine

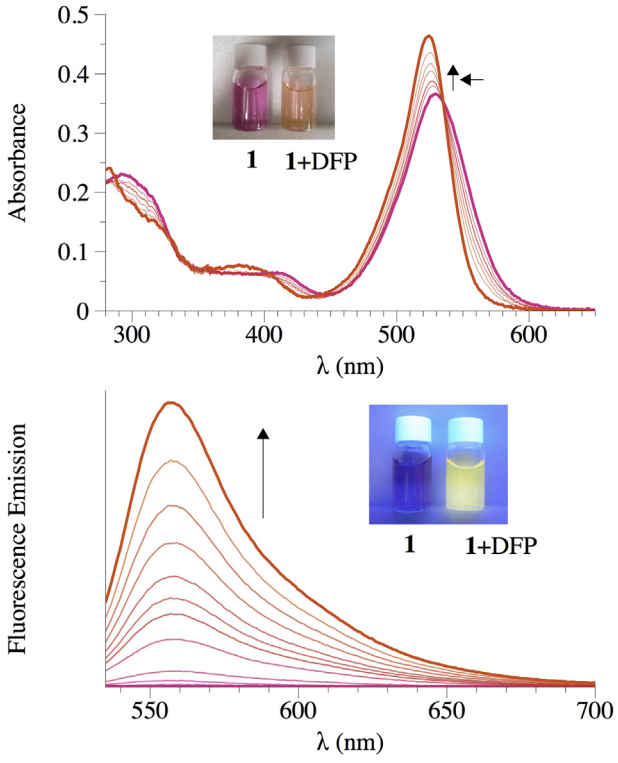

Fig. 2. UV–vis spectra (top) and emission spectra (bottom, $\lambda_{exc} = 470$ nm) of compound **1** (5×10^{-6} M in MeCN) titrated with DFP (from 5 μM to 3 mM). Insets: Observable colour changes upon addition of the simulant.

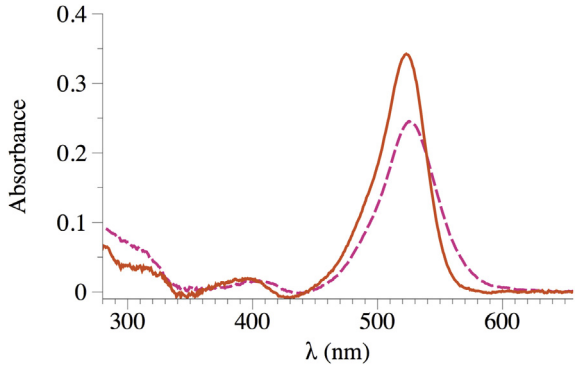

Fig. 3. UV–vis spectra of compound **1** (5×10^{-6} M in H_2O/MeCN 3/1 v/v and 100 mM MES pH 5.5) in the absence (dashed line) and presence (continuous line) of 10 mM DCNP.

6G ($\Phi_f = 0.95$ in ethanol) [23] as a standard). After protonation with TFA, this band increases 1000-fold reaching a fluorescence quantum yield of $\Phi_f = 0.639$. No shifts were observed for the emission band upon addition of TFA. The large stokes shift of **1** and **1** + H^+ if compared to **5** (25 and 31 *versus* 8 nm) indicates the charge redistribution after excitation.

The low fluorescence intensity observed for **1** can be attributed to a quenching process related to the excited ICT state. This state is essentially non emissive. After protonation with TFA, the disabling of the ICT process results in an increase of the fluorescence intensity in the locally excited state (LE). The fluorescence decay of **1** + H^+ is biexponential with short-lived and long-lived components of $\tau_1 = 0.23$ ns and $\tau_2 = 4.198$ ns.

In order to take advantage of these optical features, and use them as a signal transducer, the sensing unit was designed in such a way that in the presence of diverse organophosphate compounds its donor character irreversibly vanishes by the formation a quaternary ammonium salt (see Scheme 2) with all the optical changes that this implies.

2.3. Detection experiments in solution

Firstly, we explored the behaviour of probe **1** in the presence of the organophosphorous compounds DCNP and DFP in acetonitrile. To 5×10^{-6} M solutions of **1** in MeCN, different amounts of the simulants, ranging from 5 μM to 12 mM, were added.

Immediately, the expected changes were observed in the two optical channels: a gradual hypsochromic shift of the main absorption band, together with a strong increase of the emission band intensity occurred until a maximum concentration of 3 mM and 12 mM for DCNP and DFP respectively (see Fig. 2 for DFP). The colourimetric changes could be easily observed by the naked eye, together with the increase in the fluorescence, which was easily followed by exposing the samples under a hand-held UV lamp (Fig. 3).

In order to achieve *from lab to field* chemodosimeter, this has to be capable of detecting the analyte in more realistic samples. For instance, one of the targets of this chemodosimeter could be the detection of organophosphonates in contaminated water (*e.g.* city water supply in conflict zones), hence the need of the sensor to work in aqueous environment.

After testing several aqueous mixtures, we found our optimal conditions by using a 3/1 v/v water/acetonitrile mixture. Additionally, 100 mM 2-(*N*-morpholino)ethanesulfonic acid (MES) was employed to buffer the solution at pH 5.5, which guarantees the absence of false positives due to proton traces (*e.g.* mineral acids such as HF from the decomposition of DFP). Additionally, the buffer

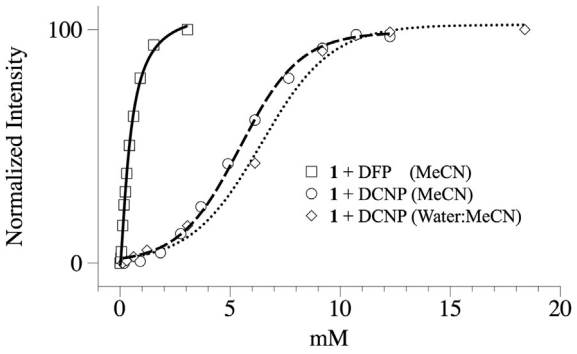

Fig. 4. Titration profiles of the emission intensity at 555 nm of **1** with DCNP and DFP in acetonitrile and with DCNP in a water-MeCN mixture.

ensures a constant ionic strength aiding to the reproducibility of the analysis. It is worth to remark the good solubility of **1** in this medium, without the need of tailoring the BODIPY core.

After addition of 5 mM of DCNP, a 10-fold increase in the emission intensity was observed, together with a hypsochromic shift. The pH of the solution remained the same, ensuring that all the achieved response was due to the selective detection of DCNP.

On the other hand, the addition of up to 10 mM of DFP to probe **1** made no changes in the optical properties of the aqueous mixture, probably due to the higher lipophilic character of this simulant that causes miscibility problems. This observation precluded the use of DFP in aqueous systems.

2.4. Kinetic studies

The kinetics of the reaction between the nerve agent simulant DCNP and probe **1** in buffered water-acetonitrile mixtures was evaluated. Different excess amounts of DCNP were added to four different samples containing probe **1** (5×10^{-6} M in H_2O/MeCN 3/1 v/v and 100 mM MES pH 5.5) in such a way that the final concentration of DCNP was 1.8, 3.6, 5.4 and 7.2 mM. The samples were placed in a multi-cell holder and the emission intensity at 555 nm was constantly monitored vs. time. As the simulant is in 300–1500-fold excess, the experiment fulfilled the conditions of the Ostwald isolation method, ensuring pseudo first-order kinetic conditions.

Plotting $\ln[(I_f - I)]$ *versus* time (in which, I_f is the final emission intensity and I is the emission intensity at a given time), allowed us the determination of the observed rate constants (k_{obs}). From the k_{obs} values and the corresponding DCNP concentrations we were able to evaluate the global constant rate (k) (Fig. 4).

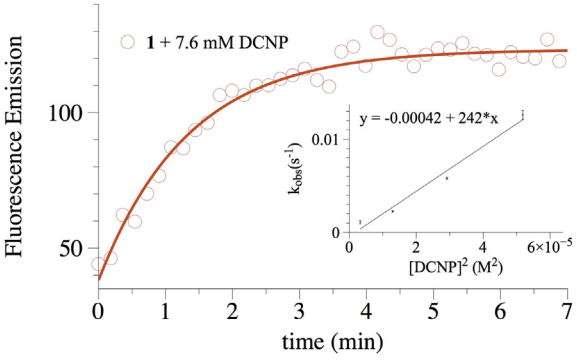

Fig. 5. Kinetic profile of the emission intensity at 555 nm of probe **1** after the addition of 7.2 mM DCNP. Probe **1** is 5×10^{-6} M water/acetonitrile 3/1 v/v mixture (pH = 5.5). The inset figure shows the correlation between k_{obs} and $[DCNP]^2$.

Fig. 5 shows the emission intensity changes of probe **1** at 555 nm for an initial DCNP concentration of 7.2 mM. The reaction is relatively fast, and maximum emission changes are observed after a few minutes. The global rate constant for **1** in the presence of DCNP was $k = 242\ M^{-2}\ s^{-1}$. The calculated half-life time of **1** in the presence of *i.e.* 7.2 mM of DCNP ($k_{obs} = 12.6 \times 10^{-3}\ s^{-1}$) was *ca* 1 min.

Additionally, kinetic experiments in pure acetonitrile were attempted too. Unfortunately, the velocity of the reaction in this solvent was too quick to be monitored by conventional methods.

2.5. Limits of detection and potential interferents

Detection limits for the reaction of the nerve agent simulants DCNP and DFP with **1** in acetonitrile or buffered water-acetonitrile mixture were evaluated. For this determination, increasing amounts of the simulants were added to 3 mL solutions of **1** until the emission values fulfilled the condition:

$$I_s = I_{blank} + 3 \times \sigma_{blank}$$

where I_s is the sample emission intensity at $\lambda_{em} = 560$ nm after 2 min of addition of the simulant, I_{blank} is the emission intensity mean of the blank and σ_{blank} is the standard deviation of the blank.

The achieved LODs were 2.7 and 1.8 ppm (v/v) for DCNP and DFP (respectively) in acetonitrile and 14 ppm (v/v) for DCNP in the buffered aqueous mixture [24].

Once more, we wanted to ensure that chemically related species and other conventional compounds present in the fields of application of this probe did not interfere rendering false positives or disabling the probe. Thus, we tested the reactivity of **1** towards other organophosphorous compounds (OP) (DECP, DPEP, DCTP, DMTP and DOPP, see Scheme 1) and pesticides (1,1-dichloro-2,2-bis(*p*-chlorophenyl)ethane (4,4′-DDD) and 1,1-dichloro-2,2-bis(*p*-chlorophenyl)ethylene (4,4′-DDE)) besides gasoline and diesel.

The test was performed contaminating buffered aqueous solutions of **1** (water/acetonitrile 3:1 v/v pH = 5.5 MES 0.1 M) with *ca.* 300 ppm of the possible interferents. None of them was able to yield a significant response on the sensor similar to that of the DCNP. The highest response was observed for DCTP which increased the fluorescence of **1** up to 7% of the maximum, probably due to the similar chemical nature to that of DCNP (see Fig. 6).

Additionally, after each test was performed, the analyte DCNP (300 ppm) was added to the contaminated aqueous mixture of **1**, reproducing an optical response similar to that of pure DCNP. These results prove not only that **1** is selective to the nerve agent simulants, but also that it is capable to detect them even inside a more complex matrix (Schemes 3 and 4).

2.6. Solid-liquid detection experiments

The sensing properties of **1** immobilized on a solid support were also evaluated, since immobilization of chemodosimeters is a key step to jump from the lab to the field in sensing applications. We decided to immobilize **1** in a hydrophilic polyurethane based matrix (Hydromed D4) due to its similarity to water environments. This matrix was later applied as a coating over polyethylene strips. After drying for 12 h, the solid material presented no observable fluorescence under a hand-held UV_{365nm} lamp. When the strips were dipped into distilled water contaminated with DCNP (from 10 to 1000 ppm_v), a strong enhancement of the fluorescence was observed by the naked eye (see Fig. 7).

After the test was performed, washing the strips with distilled water did not quench the fluorescence, indicating that the observed changes in fluorescence were due to the irreversible cyclization of **1**.

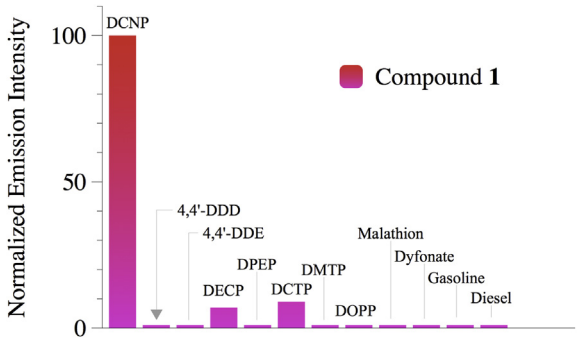

Fig. 6. Relative (to DCNP) emission intensity of **1** (measured at 560 nm) with 300 ppm (v/v) of DCNP, pesticides, OP compounds, gasoline and diesel.

As an extra experiment, tap water samples were contaminated with DCNP, and after dipping the solid material containing **1** in the sample, the same strong luminescence was observed. In addition, no luminescence was produced for non-contaminated tap-water, indicating that alkaline ions and other substances present in this liquid do not interfere with the measurement.

2.7. Detection in the gas phase

The high volatility of the nerve agent gases makes absolutely necessary for a chemodosimeter to be able to effectively perform a fast but still trustworthy detection of these compounds in the gas phase. Thus, as a simple experiment, we prepared a small assay kit by adsorbing probe **1** over commercial silica plate strips containing no fluorophore. The adsorption was performed by dipping the strip during 5 s in a 1.5×10^{-3} M acetonitrile solution of the probe.

The sensing experiment was carried out by suspending the strip in the middle of a 5 L glass round bottom flask, which was sealed with a septum. The experimental atmosphere was common air, at a relative humidity of 60–65%. The inner atmosphere was contaminated with DCNP by adding different amounts via syringe to the bottom of the flask. Within 5 min, a lightening of the sample could be observed by the naked eye, whereas the fluorescent changes were evident under UV_{365nm} light irradiation (see inset of Fig. 8).

The solid state fluorescence spectra of these strips were measured prior and after exposure to the nerve gas simulant using a 20° configuration to minimize the amount of scattered light. Prior to the exposure, the probe showed a weak fluorescence, possibly due to slight interaction with the acidic silica. After exposure to 2 ppm of DCNP, this band increased 16-fold, yielding a slightly broadened spectrum which was 10 nm red shifted when compared with the corresponding spectrum in solution (see Fig. 8).

2.7.1. Limits of detection in gas phase and interferents

With this experimental device we were able to visually detect within 1 min down to 0.2 ppm of DCNP (1 μL of DCNP spread in a 5 L flask).

The strips were also tested *versus* different gases that could be present in civilian or military setting. Thus, sensing strips containing probe **1** were exposed ozone, gasoline and diesel vapours, as well as ammonia, and exhaust pipe fumes. In all cases, negligible changes were found for the emission intensity of the strips.

3. Conclusions

We have synthesized and demonstrated the use of compound **1** as fluoro-chromogenic probe for the selective detection of the nerve agent simulants DCNP and DFP. The probe **1** is based on a 2-(2-(dimethylamino)phenyl)ethanol sensing unit using a BODIPY core as chromophore and fluorophore. We have studied its spectroscopic properties and we have found that **1** has very low fluorescence quantum yield, presumably due to a quenching by an ICT process. The probe has been designed in such a way that in the presence of the simulants, the ICT becomes cancelled. Thus, after reaction with DCNP or DFP an increase of the fluorescence intensity, along with a hypsochromic shift of the main absorption band is observed. Compound **1** is able to detect DCNP in aqueous mixtures and has proved to be selective towards nerve agent simulants in the presence of other organophosphorous compounds, pesticides, and other interferents. The probe can detect DCNP and DFP in solution in the 1–20 ppm range.

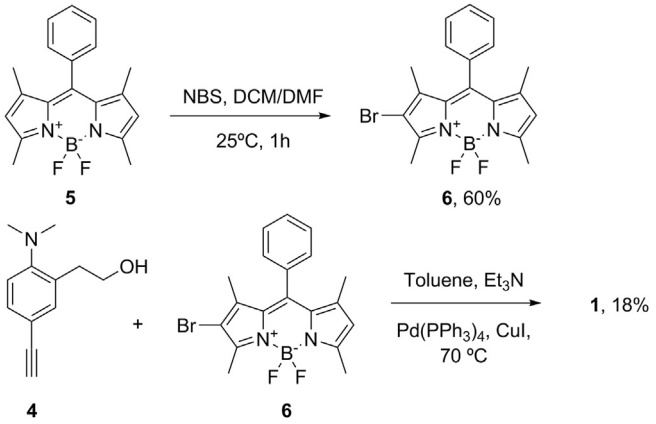

Scheme 4. Synthesis of the bromo-BODIPY precursor **6** and Sonogashira cross-coupling reaction to obtain probe **1**.

Furthermore, we have demonstrated the solid–gas detection capabilities of **1** by adsorbing the probe on solid silica matrices, and exposure to DCNP vapours reaching LODs of 0.2 ppm.

We believe that the good sensitivity and selectivity achieved by this chemodosimeter together with the photostability ascribed to the BODIPY dyes can be a great contribution for the production of trustworthy and robust portable sensing devices.

4. Experimental section

4.1. General methods

Nerve agent simulants DCNP and DFP are very toxic compounds, thus, special precautions need to be taken when

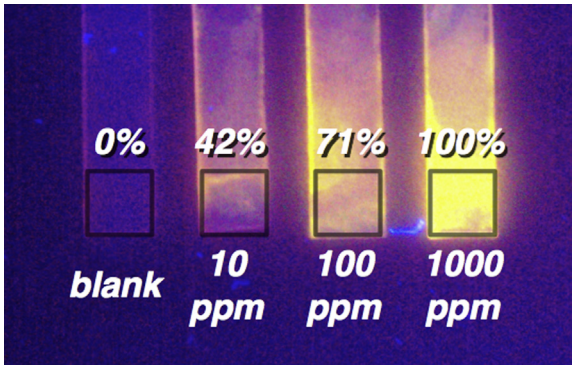

Fig. 7. Polyethylene strips coated with hydromed previously doped with compound **1**. The strips were dipped in distilled water contaminated with 0, 10, 100 and 1000 ppm_v of DCNP. Top values indicate the relative (to the rightmost strip) luminance of the measured squared areas. Measurement was carried out by meaning the CIE luminance of all the pixels inside the squared area with custom-made image processing software.

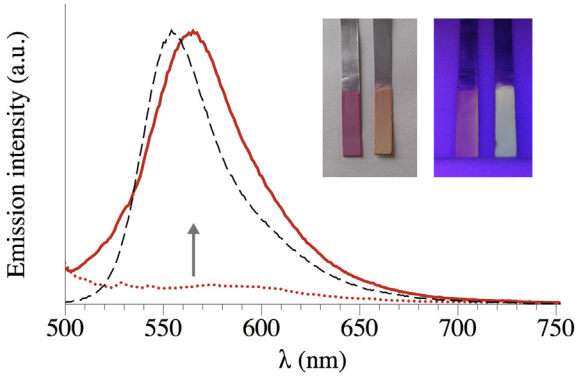

Fig. 8. Solid state fluorescence spectrum (λ_{exc} = 480 nm) of compound **1** over silica plates in the absence (dotted line) and in the presence (continuous line) of 2 ppm atmosphere of DCNP (2 μL of DCNP spread in a 1 L flask). Additionally, dashed line shows normalized spectra in of **1** + DCNP in acetonitrile. The inset picture shows the prepared silica strips of (from left to right) **1**, **1** + 2 ppm DCNP and both samples under UV_{365nm} light.

performing any experiment with them. Manipulations involving DCNP or DFP were performed in a glove box with constant air flow. The stream coming from the glove box exhaust was bubbled in a saturated NaOH water solution placed inside the fume hood. UV–vis and fluorescence measurements were performed with tight capped cuvettes previously prepared in the glove box. In the cases were the experimental setup was too large to be fitted in the glove box, the experiment was performed in the fume-hood under special precautions.

All the synthetic manipulations were performed in a dry argon atmosphere using standard techniques. Compound **5** was prepared according to the procedures described in the literature [20]. Tetrahydrofuran was distilled over Na prior to use. The other materials were purchased and used as received. Silica gel 60 F254 (Merck) plates were used for TLC. ^{1}H and ^{13}C NMR spectra were recorded using a Bruker DRX-500 spectrometer (500 MHz for ^{1}H and 126 MHz for ^{13}C) and a Bruker Avance 400 MHz (400 MHz for ^{1}H and 100 MHz for ^{13}C) with the deuterated solvent as the lock and residual solvent as the internal reference. HRMS were recorded using a Shimadzu QP5050A. Absorption spectra were recorded with a Shimadzu UV-2101PC spectrophotometer. Fluorescence spectra were carried out in a Varian Cary Eclipse fluorimeter.

4.2. Preparation of the hydrogel coated polyethylene films

Polyurethane based hydrogel (Hydromed D4®) (4.0 g) was mixed by 1 h rotation with EtOH (55 mL) and water (4.8 mL). To 2.5 mL of the viscous solution, an acetonitrile solution of **1** (1.5 mM, 500 μL) was added, and the resulting mixture was again rotated for an additional hour.

Transparent polyethylene strips (45 × 6 × 0.5 mm) were then dipped once in the solutions. The excess of hydrogel solution was removed and the strips were allowed to dry at room temperature for 2 h.

4.3. Preparation of the silica doped strips

Commercial silica gel over aluminium foil without fluorescent indicator (Sigma Aldrich) were cutted in 45 × 6 mm strips and then dipped for 10 s in a 1.5 mM solution of **1**. The strip was allowed to dry at room temperature for 30 min. Additionally, part of the silica was removed from the aluminium plate in such a way that the active area shaped a 20 × 6 mm rectangular surface.

4.4. Experimental procedures

4.4.1. Synthesis of *1*

BODIPY **6** (80 mg, 0.2 mmol) was dissolved in a toluene/Et_3N 2/1 v/v mixture (20 mL), under an argon atmosphere. The mixture was sparged with argon for 10 min. Then, CuI (1.9 mg, 5 mol%) and tetrakis(triphenylphosphine)palladium(0) (11.5 mg, 5 mol%) were added, and the acetylene derivative **4** was added dissolved in the minimum amount of previously degassed toluene. The reaction was sparged with argon for 10 more min. Then, the mixture was heated to 70 °C and allowed to react for 24 h. After this time, solvents were evaporated and the mixture was then dissolved in DCM. The organic solvent was washed twice with water, and the aqueous layer was extracted with DCM. The combined organic layers were washed with aq NaCl (sat.) and dried with $MgSO_4$. After solvent evaporation, the remaining mixture was purified by silica column chromatography using EtOAc–hexane 2:8 as eluent to yield a dark red solid (18 mg, 18%). ^{1}H NMR (500 MHz, CD_2Cl_2) δ 7.57 (dd, J = 5.1, 2.0 Hz, 3H), 7.38–7.34 (m, 3H), 7.31 (d, J = 2.0 Hz, 1H), 7.16 (d, J = 8.2 Hz, 1H), 6.12 (s, 1H), 3.83 (t, J = 5.8 Hz, 2H), 2.98 (t, J = 5.9 Hz, 2H), 2.73 (s, 6H), 2.69 (s, 3H), 2.59 (s, 3H), 1.55 (s, 3H), 1.45 (s, 3H). ^{13}C NMR (126 MHz, CD_2Cl_2) δ 157.58, 156.13, 152.60, 144.94, 142.49, 142.28, 135.78, 134.57, 133.64, 132.44, 130.37, 130.21, 129.26, 129.13, 127.93, 122.00, 119.86, 119.29, 115.14, 95.69, 81.15, 63.81, 44.58, 35.61, 14.48, 14.27, 13.26, 12.90. HR-MS: calcd for $C_{31}H_{33}N_3OF_2B$ $[M + H]^+$: 512.2679, found: 512.2685.

4.4.2. Synthesis of compound *6*

BODIPY **5** (1 g, 3.08 mmol) was dissolved in a DMF/DCM 2/1 v/v mixture (150 mL). Then, *N*-bromosuccinimide (660 mg, 3.69 mmol) dissolved in DCM (50 mL) was added slowly. After one hour, the reaction mixture was washed three times with water, followed by a washing step with brine. The organic phase was dried with $MgSO_4$, and after evaporation of the solvent, the red solid was purified with silica gel column chromatography using hexane–DCM (1:9 → 4:6) as eluent. Yield: 60% (726 mg).

Rf = 0.52 (EtOAc hexane 1:9). ^{1}H NMR (500 MHz, $CDCl_3$) δ 7.55–7.51 (m, 3H), 7.31–7.27 (m, 2H), 6.06 (s, 1H), 2.62 (s, 3H), 2.60 (s, 3H), 1.41 (s, 3H), 1.39 (s, 3H). ^{13}C NMR (126 MHz, $CDCl_3$) δ 157.93, 151.46, 145.10, 141.84, 138.77, 134.67, 132.04, 129.82, 129.28, 129.25, 127.87, 122.16, 110.62, 14.77, 14.55, 13.47, 13.40. HR-MS: calcd for $C_{19}H_{17}BBrF_2N_2$ $[M + H]^+$: 403.0787, found: 403.0791.

4.4.3. Synthesis of compound *2*

2-(2-Nitrophenyl)ethanol (10 g, 61 mmol), formaldehyde (37%, 11.24 mL, 75.2 mmol), ethanol (200 mL), and Pd/C (500 mg, 10%) were placed under an H_2 atmosphere at 60 PSI until the uptake of hydrogen ceased. After filtration through celite, the solvent was evaporated, and the residue was dissolved in EtOAc, and washed twice with water, and aq NaCl (sat.). The organic phase was dried using $MgSO_4$, and the solvent was evaporated to give 2-(2-(N,N-dimethylamino)phenyl)ethanol as crude oil. The oil (10.12 g, 61 mmol) and ammonium acetate (470 mg, 6.1 mmol) were dissolved in acetonitrile (300 mL) in a round bottom flask. Then, the mixture was cooled down to 0 °C, and a solution of N-bromosuccinimide (10.85 g, 61 mmol) in acetonitrile (10 mL) was added dropwise. After 1 h, the solvent was evaporated and the mixture dissolved in EtOAc. The organic solvent was washed twice with 10% Na_2CO_3 and sat. aq NaCl. The organic phase was dried with $MgSO_4$ and evaporated. The remaining oil was purified by silica column chromatography using EtOAc–hexane 4:6 as eluent to yield brownish oil (10.61 g, 71% overall yield). Rf = 0.77 (EtOAc: hexane 6:4). ^{1}H NMR (500 MHz, $CDCl_3$) δ 7.24 (dd, J = 8.5, 2.4 Hz, 1H), 7.21 (d, J = 2.3 Hz, 1H), 6.97 (d, J = 8.5 Hz, 1H), 3.75 (*t*, J = 5.7 Hz, 2H), 2.87 (*t*, J = 5.7 Hz, 2H), 2.59 (s, 6H). ^{13}C NMR (125 MHz, $CDCl_3$)

δ 151.36, 138.22, 133.64, 130.35, 121.77, 117.61, 77.00, 63.86, 44.81, 35.61. HR-MS: calcd for $C_{10}H_{14}BrNO$ $[M + H]^+$: 244.0337, found: 244.0341.

4.4.4. Synthesis of compound **3**

Compound **2** (4.15 g, 17.0 mmol) was dissolved in a toluene/Et_3N 2:1 v/v mixture (75 mL) in a three-neck round bottom flask. The inner atmosphere was evacuated and replaced with argon. This operation was repeated two more times. Then, the mixture was sparged with argon for 10 min. After this time, tetrakis(-triphenylphosphine)palladium(0) (982 mg, 5 mol%) and copper(I) iodide (162 mg, 5 mol%) were added to the reaction mixture with the help of toluene (10 mL). After 10 more min of sparging with argon, trimethylsilaneacetylene (2.0 g, 20.4 mmol) dissolved in degassed toluene (20 mL) was added and the temperature was raised to 50 °C. The mixture was allowed to react for 72 h. After the reaction cooled down, DCM was added to the mixture and then it was washed three times with 10% aq NH_4Cl. The aqueous layers were reunited, and extracted with DCM. The combined organic layers were washed with brine, dried with $MgSO_4$ and evaporated. The residue was purified with silica gel column chromatography using EtOAc–hexane 2:8 as eluent, which yielded **3** as yellowish oil (3.07 g, 69%). R_f = 0.41 (EtOAc–hexane 4:6). ^1H NMR (500 MHz, $CDCl_3$) δ 7.33 (dd, J = 8.3, 2.0 Hz, 1H), 7.28 (d, J = 2.0 Hz, 1H), 7.09 (d, J = 8.2 Hz, 1H), 3.83 (t, J = 5.6 Hz, 2H), 2.97 (t, J = 5.7 Hz, 2H), 2.72 (s, 6H), 0.24 (s, 9H). ^{13}C NMR (126 MHz, $CDCl_3$) δ 151.92, 135.70, 134.76, 131.37, 119.78, 117.08, 104.70, 93.85, 64.18, 44.96, 35.87, 0.00. HR-MS: calcd for $[M + H]^+$ $C_{15}H_{24}NOSi$: 262.1621, found: 262.1617.

4.4.5. Synthesis of compound **4**

Compound **3** (254 mg, 0.97 mmol) was dissolved in MeOH (10 mL). Then, K_2CO_3 (1.34 g, 9.7 mmol) was added to the mixture. After 30 min, thin layer chromatography revealed complete deprotection. Then, water was added, and a solution of 0.1 M HCl was slowly added until neutralization. Then, the mixture was extracted three times with DCM, the organic layers were combined and washed with brine, dried with $MgSO_4$ and evaporated. The product (169 mg, 92%) was used without further purification. R_f = 0.34 (EtOAc–hexane 4:6). ^1H NMR (500 MHz, $CDCl_3$) δ 7.38 (dd, J = 8.2, 2.1 Hz, 1H), 7.32 (d, J = 2.0 Hz, 1H), 7.13 (d, J = 8.2 Hz, 1H), 3.86 (t, J = 5.7 Hz, 2H), 3.05 (s, 1H), 2.99 (t, J = 5.7 Hz, 2H), 2.73 (s, 6H). ^{13}C NMR (126 MHz, $CDCl_3$) δ 152.76, 135.89, 134.81, 131.55, 119.93, 118.38, 83.37, 76.74, 64.17, 44.83, 35.83. HR-MS: calcd for $C_{12}H_{16}NO$ $[M + H]^+$: 190.1226, found: 190.1227.

Acknowledgements

We thank the Spanish Government and the European FEDER funds (project MAT2012-38429-C04-02 and 01). SCSIE and ICMOL (Universidad de Valencia) are gratefully acknowledged for all the equipment employed. R.G. is grateful to the Spanish Ministry of Education for its FPU grant. Knut Rurack is gratefully acknowledged for the life-time measurements performed at his lab.

References

[1] Okumura T, Takasu N, Ishimatsu S, Miyanokim S, Mitsuhashi A, Kumada K, et al. Report on 640 victims of the Tokyo subway Sarin attack. Ann Emerg Med 1996;28:129–35.

[2] Abu-Qare AW, Abou-Donia MB. Sarin: health effects, metabolism, and methods of analysis. Food Chem Toxicol 2002;40:1327;
Wang J, Gu J, Leszczynski J. Phosphonylation mechanisms of Sarin and acetylcholinesterase: a model DFT study 2006;110:7567–73.

[3] Sidell FR, Groff WA. The reactivatibility of cholinesterase inhibited by VX and Sarin in man. Toxicol Appl Pharmcol 1974;27:241–52;
Jokanović M, Prostran M. Pyridinium oximes as cholinesterase reactivators. Structure-activity relationship and efficacy in the treatment of poisoning with organophosphorus compounds. Curr Med Chem 2009;16:2177–88.

[4] Roscioli KM, Lamabadusuriya MR, Harden CS, Midey AJ, Wu C, Siems WF, et al. Structure selective ion molecule interactions (SSIMI) in ion mobility spectrometry. Int J Ion Mobil Spectrom; 2013:1–11;
Maziejuk M, Ceremuga M, Szyposzyńska M, Sikora T. Effect of temperature on separation of Sarin (GB) ions in differential mobility spectrometry. Open J Phys Chem 2013;3:170–6.

[5] Seto Y, Kanamori-Kataoka M, Tsuge K, Ohsawa I, Iura K, Itoi T. Sensitive monitoring of volatile chemical warfare agents in air by atmospheric pressure chemical ionization mass spectrometry with counter-flow introduction. Anal Chem 2013;85:2659–66.

[6] Ringer JM. Detection of nerve agents using proton transfer reaction mass spectrometry with ammonia as reagent gas. Eur J Mass Spectrom 2013;19:175–85.

[7] Pohanka M. Cholinesterases in biorecognition and biosensors construction: a review. Anal Lett 2013;46:1849–68;
Pohanka M, Adam V, Kizek R. An acetylcholinesterase-based chronoamperometric biosensor for fast and reliable assay of nerve agents. Sensors 2013;13:11498–506;
Dhull V, Gahlaut A, Dilbaghi N, Hooda V. Acetylcholinesterase biosensors for electrochemical detection of organophosphorus compounds: a review. Biochem Res Int 2013;2013:731501.

[8] Ge X, Tao Y, Zhang A, Lin Y, Du D. Electrochemical detection of dual exposure biomarkers of organophosphorus agents based on reactivation of inhibited cholinesterase. Anal Chem 2013;85:9686–91;
Tan HY, Loke WK, Nguyen NT, Tan SN, Tay NB, Wang W, et al. Lab-on-a-chip for rapid electrochemical detection of nerve agent Sarin. Biomed Microdevices; 2013:1–7;
Sahin A, Dooley K, Cropek DM, West AC, Banta S. A dual enzyme electrochemical assay for the detection of organophosphorus compounds using organophosphorus hydrolase and horseradish peroxidase. Sens Actuators B Chem 2011;158:353–60;
Delalande M, Clavaguera S, Toure M, Carella A, Lenfant S, Deresmes D, et al. Chemical functionalization of electrodes for detection of gaseous nerve agents with carbon nanotube field-effect transistors. Chem Commun 2011;47:6048–50.

[9] Yang Y, Ji H, Thundat T. Nerve agents detection using a Cu^{2+}/L-cysteine bilayer-coated microcantilever. J Am Chem Soc 2003;125:1124–5;
Zhao Q, Zhu Q, Shih WY, Shih WH. Array adsorbent-coated lead zirconate titanate (PZT)/stainless steel cantilevers for dimethyl methylphosphonate (DMMP) detection. Sens Actuators B Chem 2006;117:74–9.

[10] Liu F, Huang S, Xue F, Wang Y, Meng Z, Xue M. Detection of organophosphorus compounds using a molecularly imprinted photonic cristal. Biosens Bioelectron 2012;32:273–7;
He W, Liu Z, Du X, Jiang Y, Xiao D. Analytical application of poly{methyl[3-(2-hydroxy-3,4-difluoro)phenyl]propyl siloxane} as a QCM coating for DMMP detection. Talanta 2008;76:698–702.

[11] Aernecke MJ, Walt DR. Optical-fiber arrays for vapor sensing. Sens Actuators B Chem 2009;142:464–9.

[12] Wang F, Gu H, Swager TM. Carbon nanotube/polytiophene chemiresistive sensors for chemical warfare agents. J Am Chem Soc 2008;130:5392–3;
Claveguera S, Raoul N, Carella A, Delalande M, Celle C, Simonato J-P. Development of an autonomous detector for sensing of nerve agents based on functionalized silicon nanowire field-effect transistors. Talanta 2011;85:2542–5;
Claveguera S, Carella A, Caillier L, Celle C, Pécaut J, Lenfant S, et al. Sub-ppm detection of nerve agents using chemically functionalized silicon nanoribbond field-effect transistors. Angew Chem Int Ed 2010;49:4063–6;
Kwon OS, Park SJ, Lee JS, Park E, Kim T, Park H-W, et al. Multidimensional conducting polymer nanotubes for ultrasensitive chemical nerve agent sensing. Nano Lett 2012;12:2797–802;
Wei L, Shi D, Ye P, Dai Z, Chen H, Chen C, et al. Hole doping and surface functionalization of single-walled carbon nanotube chemiresistive sensors for ultrasensitive and highly selective organophosphor vapor detection. Nanotechnology 2011;22:425501–7.

[13] Costero AM, Parra M, Gil S, Gotor R, Mancini PM, Martínez-Máñez R, et al. Chromo-fluorogenic detection of nerve-agent mimics using triggered cyclization reactions in push-pull dyes. Chem Asian J 2010;5:1573–85;
Costero AM, Parra M, Gil S, Gotor R, Mancini PM, Martínez-Máñez R, et al. Selective detection of nerve agent simulants by using triarylmethanol-based chromogenic chemodosimeters. Eur J Org Chem 2012;26:4937–46;
Ajami D, Rebek Jr J. Chemical approaches for detection and destruction of nerve agents. Org Biomol Chem 2013;11:3936–42.

[14] Dale TJ, Rebek J. Fluorescent sensors for organophosphorus nerve agent mimics. J Am Chem Soc 2006;128:4500–1;
Zhang S, Timothy MS. Fluorescent detection of chemical warfare agents: functional group specific ratiometric chemosensors. J Am Chem Soc 2003;125:3420–1.

[15] Xuan W, Cao Y, Zhou J, Wang W. A FRET-based ratiometric fluorescent and colorimetric probe for the facile detection of organophosphonate nerve agent mimic DCP. Chem Commun 2013;49:10474–6.

[16] Martí A, Costero AM, Gaviña P, Gil S, Parra M, Brotons-Gisbert M, et al. Functionalized gold nanoparticles as an approach to the direct colorimetric detection of DCNP nerve agent simulant. Eur J Org Chem 2013;22:4770–9;

Liu D, Chen W, Wei J, Li X, Wang Z, Jiang X. A highly sensitive, dual-readout assay based on gold nanoparticles for organophosphorus and carbamate pesticides. Anal Chem 2012;84:4185–91;
Lee JS, Shin DH, Jun J, Jang J. Multidimensional polypyrrole/iron oxyhydroxide hybrid nanoparticles for chemical nerve gas agent sensing. ACS Nano 2013;7:10139–47;
Sun J, Guo L, Bao Y, Xie J. A simple, label-free AuNPs-based colorimetric ultrasensitive detection of nerve agents and highly toxic organophosphate pesticide. Biosens Bioelectron 2011;28:152–7.

[17] Ordronneau L, Carella A, Pohanka M, Simonato J-P. Chromogenic detection of Sarin by discolouring decomplexation of a metal coordination complex. Chem Commun 2013;49:8946–8.

[18] Chulvi K, Gaviña P, Costero AM, Parra M, Gil S, Gotor R, et al. Discrimination of nerve gases mimics and other organophosphorous derivatives in gas phase using a colorimetric probe array. Chem Commun 2012;48:10105–7.

[19] Loudet A, Burgess K. BODIPY dyes and their derivatives: syntheses and spectroscopic properties. Chem Rev 2007;107:4891–932.

[20] Kollmannsberger M, Rurack K, Resch-Genger U, Daub J. Ultrafast charge Transfer in amino-substituted boron dipyrromethene dyes and its inhibition by cation complexation: a new design concept for highly sensitive fluorescent probes. J Phys Chem A 1998;102:10211–20.

[21] Wagner S, Brödner K, Coombs BA, Bunz UHF. Pyridine-substituted BODIPY as fluorescent probe for Hg^{2+}. Eur J Org Chem 2012;11:2237–42;
Wang Y, Zhang D, Zhou H, Ding J, Chen Q, Xiao Y, et al. Nonlinear optical properties and ultrafast dynamics of three novel boradiazaindacene derivatives. J Appl Phys 2010;108:033520;
He H, Ng DKP. A ratiometric near-infrared pH-responsive fluorescent dye based on distyryl BODIPY. Org Biomol Chem 2011;9:2610–3;
Bonardi L, Ulrich G, Ziessel R. Tailoring the properties of boron–dipyrromethene dyes with acetylenic functions at the 2,6,8 and 4-B substitution positions. Org Lett 2008;10:2183–6.

[22] Niua S, Ulrich G, Retailleau P, Ziessel R. BODIPY-bridged push–pull chromophores: optical and electrochemical properties. Tetrahedron Lett 2011;52:4848–53;
Bonnier C, Machin DD, Abdi O, Koivisto BD. Manipulating non-innocent π-spacers: the challenges of using 2,6-disubstituted BODIPY cores within donor–acceptor light-harvesting motifs. Org Biomol Chem 2013;11:3756–60.

[23] Kubin RF, Fletcher AN. Fluorescence quantum yields of some rhodamine dyes. J Lumin 1982;27:455–62.

[24] The US Enviromental Protection Agency (EPA) states that the Sarin's LD50 for humans averaging 70 kg is 12 mg.